A MULTIAXIAL CONSTITUTIVE MODEL FOR CONCRETE IN THE FIRE SITUATION

Thomas Gernay* & Jean-Marc Franssen**
*The National Fund for Scientific Research, Belgium
**University of Liege, Belgium

ABSTRACT

Performance-based design in fire engineering leads to increasing demand for advanced temperature-dependent material models for the load bearing materials used in building structures. These models must be valid in natural fire situations including cooling down phase and must be sufficiently robust for complex numerical calculations such as, for example, the analysis of tensile membrane action in composite slabs. Although structural concrete is widely used in civil engineering, proper modelling of its thermo-mechanical behaviour remains a challenging issue for engineers mainly because of the complexity of the phenomena that result from the microcracking process in this material and because of the necessity to ensure the numerical robustness of the models.

This paper presents a new multiaxial concrete model based on a plastic-damage formulation and developed to meet the specific requirements of structural fire engineers and researchers. The model, which incorporates an explicit term for transient creep strain and encompasses a limited number of material parameters, has been implemented in a finite element software dedicated to the nonlinear analysis of structures in fire. The paper presents a series of numerical simulations conducted to highlight the model ability to capture the main phenomena that develop in concrete under fire (permanent strains, degradation of the elastic properties, unilateral effect) as well as its ability to be used for the fire analysis of large-scale structural elements. As an example, the new concrete model is used in the numerical analysis of a full scale fire test on a composite steel-concrete slab and it is shown that the computed and measured results agree.

INTRODUCTION

In performance-based analysis, the response of structures subjected to thermo-mechanical loading is assessed by temperature-dependent calculations. These calculations require a general stress-strain relationship for modelling the behaviour of concrete at elevated temperatures. The concrete model should be reliable, accurate and numerically robust. Indeed, accuracy and reliability are required to ensure that the model captures properly the behaviour of the concrete material in all the situations of stress and temperature in the applicability domain. In addition, numerical robustness is necessary because otherwise the model cannot be used in complex and large-scale engineering problems. Finally, the model should contain a limited number of parameters that can be identified from elementary tests. The present research aims at developing a multiaxial model able to reproduce the phenomenological behaviour of concrete at elevated temperature and satisfying to the requirements of structural fire engineers.

The behaviour of concrete at the macroscopic level results from the initiation and growth of microcracks in the cementitious matrix. The microcracking process causes softening behaviour, stiffness degradation and unilateral effect. These observed phenomena can be captured by models within the framework of continuum damage mechanics. On the other hand, concrete exhibits inelastic volumetric expansion in compression, referred to as dilatancy in the literature. Proper modelling of dilatancy is very important for simulating concrete structures under multiaxial loading[1]. Dilatancy can be modelled by the development of plastic strains in concrete. Therefore, combination of the elastoplasticity theory with the damage theory results in an efficient strategy for modelling the mechanical behaviour of concrete.

Constitutive models for concrete at ambient temperature based on plastic-damage formulation have been proposed by several authors. Although concrete experiences different microcracking in different directions, models developed for structural applications usually combine plasticity with isotropic damage[1,2,3], in order to avoid the inherent complexities of numerical algorithms required by most of the anisotropic damage models[4,5]. In order to capture properly the isotropic state of damage in concrete, it is necessary to use two damage scalars and a fourth-order projection tensor. Indeed, two damage scalars are required because of the experimentally observed different damage mechanisms developing in tension and in compression[1], whereas a projection tensor is required to capture the unilateral effect[5,6].

Stress-based plasticity may be formulated either in the effective stress space[1,2,5] or in the nominal (damaged) stress space[3,7]. Effective stress is meant as the average micro-level stress applied to the undamaged volume of the material whereas nominal stress is meant as the macro-level stress and is defined as force divided by the total area. Formulation of the plastic response in the effective stress space relies on the assumption that plastic flow occurs in the undamaged material micro-bounds by means of effective quantities[8]. This formulation allows for decoupling the plastic part from the damage part in the computation process; computation of the plastic response then constitutes a standard elastoplastic problem in the effective stress space. As a result, the combination of stress-based plasticity formulated in the effective stress space and isotropic damage constitutes an interesting approach for modelling the behaviour of concrete.

Elevated temperatures are the cause of degradations at the micro-level that result in loss of stiffness and strength of the material. The thermo-mechanical model for concrete should incorporate these effects, in addition with the thermal strains and transient creep strains that develop in heated concrete. Physically, the transient creep strain is the difference in strain between concrete that is heated under load and concrete that is loaded at elevated temperature; this strain develops during first-time heating and is irrecoverable[9]. Due to the high complexity of the many phenomena involved, few multiaxial models have been proposed for the thermo-mechanical behaviour of concrete. An interesting contribution has been proposed by Nechnech *et al.*[10], who developed a plastic-damage model in plane stress state for concrete at high temperature. However, this latter model has several limitations and it has not been applied to practical problems of structural fire engineering. Research efforts are still required to give further insight into concrete modelling at elevated temperature and to extend the latest developments of ambient temperature models to elevated temperature; this is the purpose of the present study.

PRESENTATION OF THE MODEL

A general presentation of the new concrete model is presented in this section. For more detailed information, the reader should report to the thesis[11].

Assumptions

The mechanical behaviour of concrete at elevated temperatures is captured by constitutive relationships between the total strain tensor and the stress tensor. The total strain $\underline{\underline{\varepsilon}}_{tot}$ is decomposed into free thermal strain $\underline{\underline{\varepsilon}}_{th}$, transient creep strain $\underline{\underline{\varepsilon}}_{tr}$, elastic strain $\underline{\underline{\varepsilon}}_{el}$ and plastic strain $\underline{\underline{\varepsilon}}_{p}$ according to Eq. [1].

$$\underline{\underline{\varepsilon}}_{tot} = \underline{\underline{\varepsilon}}_{th} + \underline{\underline{\varepsilon}}_{tr} + \underline{\underline{\varepsilon}}_{el} + \underline{\underline{\varepsilon}}_{p} \qquad [1]$$

The sum of the elastic strain and the plastic strain is referred to as instantaneous stress-related strain $\underline{\underline{\varepsilon}}_{\sigma}$. Basic creep strain is not taken into account here but this term could easily be added to the strain decomposition.

The characterization of plastic response is formulated in the effective stress space. The elastic strain tensor is related to the effective stress tensor $\bar{\underline{\underline{\sigma}}}$ by means of the fourth-order isotropic linear-elastic stiffness tensor $\underline{\underline{\underline{\underline{C}}}}_0$, see Eq. [2].

$$\bar{\underline{\underline{\sigma}}} = \underline{\underline{\underline{\underline{C}}}}_0 : \underline{\underline{\varepsilon}}_{el} = \underline{\underline{\underline{\underline{C}}}}_0 : \left(\underline{\underline{\varepsilon}}_{\sigma} - \underline{\underline{\varepsilon}}_p \right) \qquad [2]$$

The plastic response accounts for the development of irreversible strains in the material. Yet, the degradation of the elastic properties resulting from the development of microcracks is not addressed at this stage; the unloading stiffness in the effective stress space remains equal to the isotropic linear-elastic stiffness.

Concrete exhibits different damage mechanisms in tension and in compression. In this model, a tensile damage scalar and a compressive damage scalar are adopted to capture the phenomenological effects induced by microcracking in concrete under tension and compression, respectively. Based on the work by Wu *et al.*[5], these two damage scalars lead to a fourth-order damage tensor employed to characterize the state of isotropic damage in concrete. The use of a fourth-order damage tensor allows for appropriate description of the unilateral effect inherent to concrete behaviour. Mapping of the effective stress $\bar{\underline{\underline{\sigma}}}$ into the nominal stress $\underline{\underline{\sigma}}$ is performed by this fourth-order isotropic damage tensor $\underline{\underline{\underline{\underline{D}}}}$ according to Eq. [3], where $\underline{\underline{\underline{\underline{I}}}}$ is the fourth-order identity tensor.

$$\underline{\underline{\sigma}} = \left(\underline{\underline{\underline{\underline{I}}}} - \underline{\underline{\underline{\underline{D}}}} \right) : \bar{\underline{\underline{\sigma}}} \qquad [3]$$

It is assumed that the plasticity and damage phenomena are coupled and evolve simultaneously in the material; therefore, the two phenomena are driven by the same internal variables in the model.

Finally, the new concrete model is a fully-3D constitutive model that can be used with solid finite elements or with shell finite elements; in the latter case, the plane stress version of the model is used.

Plasticity

A composite yield surface is used for capturing the concrete non-symmetrical behaviour in tension and in compression; a Rankine yield criterion is used to limit the tensile stresses and a Drucker-Prager yield contour is used for compression. The equations of the composite yield surface are written in terms of effective stresses, see Eq. [4].

$$f_t \left(\bar{\underline{\underline{\sigma}}}, \kappa_t \right) \leq 0 \quad ; \quad f_c \left(\bar{\underline{\underline{\sigma}}}, \kappa_c \right) \leq 0 \qquad [4]$$

In Eq. [4], κ_t and κ_c are the tensile and compressive hardening parameters, respectively.

Plastic flow rules have to be postulated to govern the evolution of plastic flow when the effective stress state reaches the yield surfaces. As concrete is a frictional material, in which dilatancy occurs when loaded in compression, a non-associated flow rule is adopted in compression. The plastic flow rules, in combination with the Kuhn-Tucker and consistency conditions, allow for calculation of the accumulated plastic strains in tension and compression; these accumulated plastic strains are chosen as internal variables in the model. The hardening parameters depend on the accumulated plastic strains and therefore are induced by plastic flow; these hardening parameters govern the evolution of the yield surface through the definition of the hardening laws.

Damage

The isotropic state of damage of concrete is addressed by a fourth-order damage tensor which is calculated from the tensile damage scalar d_t and the compressive damage scalar d_c as given by Eq. [5]. In this equation, the fourth-order projection tensors based on the eigenvalues and eigenvectors of the effective stress tensor are noted $\underset{\equiv\equiv}{P}^{+}$ and $\underset{\equiv\equiv}{P}^{-}$.

$$\underset{\equiv\equiv}{D} = d_t \, \underset{\equiv\equiv}{P}^{+} + d_c \, \underset{\equiv\equiv}{P}^{-} \qquad [5]$$

The projection tensors allow for a decomposition of the effective stress tensor into positive and negative components. As a result, the tensile damage scalar only affects the positive part of the effective stress tensor whereas the compressive damage scalar only affects the negative part of the effective stress tensor. Hence, the unilateral effect is captured without the need for an additional parameter.

By assumption, damage mechanism is coupled to plasticity in the model. Consequently, there is no specific threshold for damage and the evolution laws for tensile and compressive damage are driven by the accumulated plastic strains (in tension and compression, respectively). Once convergence has been obtained in the plastic return mapping algorithm, update of the damage variables is thus an explicit calculation.

Transient Creep Strain

In the numerical calculation process, computation of the increment in transient creep strain is performed at the beginning of the time step *(s)*, separately from the computation of elastic and plastic strains. The Explicit Transient Creep (ETC) Eurocode model, developed at University of Liege for uniaxial relationships[12,13], is extended to the multiaxial case by adopting the methodology proposed by de Borst and Peeters[14], see Eq. [6]. In Eq. [6], f_{ck} is the compressive strength at 20°C; the function $\Phi(T)$ is the transient creep function given in Table 1 and the fourth order tensor $\underset{\equiv\equiv}{H}$ is given by Eq. [7]. The material parameter γ that appears in Eq. [7] can be taken equal to Poisson's ratio[10], in accordance with Thelandersson's multiaxial data[15].

Accordingly, it is assumed that the process of transient creep does not induce any anisotropy. The negative part of the effective stress tensor is considered in Eq. [6] because, on the one hand, transient creep strain is assumed to occur only in compression and, on the other hand, this mechanism occurs in the undamaged part of the material.

$$\Delta \underset{=}{\varepsilon}_{tr} = \left[\phi\left(T^{(s)}\right) - \phi\left(T^{(s-1)}\right) \right] \left[\underset{\equiv\equiv}{H} \otimes \left(\underset{=}{\bar{\sigma}}^{-} \right)^{(s-1)} \Big/ f_{ck} \right] \qquad [6]$$

$$H_{ijkl} = -\gamma \, \delta_{ij} \, \delta_{kl} + 0.5\left(1+\gamma\right)\left(\delta_{ik} \, \delta_{jl} + \delta_{il} \, \delta_{jk}\right) \qquad [7]$$

Table 1. Transient creep function $\Phi(T)$.

T [°C]	20	100	200	400	600	800
Φ [-]	0.0000	0.0010	0.0018	0.0049	0.0274	0.0733

Computation of the transient creep strain increment takes into account the stress-temperature history. Between step *(s)* and *(s-1)*, there is an increment in transient creep strain, which value is computed by Eq. [6], if and only if the three following conditions are fulfilled: the temperature has increased between step *(s)* and *(s-1)*, the negative part of the (converged) effective stress at time *(s-1)* is non-null, and the material is in the ascending branch of the constitutive relationship. It is thus assumed that the positive part

of the effective stress tensor does not induce transient creep strain. Besides, the transient creep strain is irreversible at both load and temperature decrease.

Model Parameters

The model contains ten material parameters that can be obtained at ambient temperature by three basic tests: uniaxial compression test until failure comprising one unloading-reloading at peak stress, biaxial compression test until peak stress, and uniaxial tension test until failure.

Concrete subjected to elevated temperatures exhibits thermo-mechanical degradation of its properties of strength and stiffness; this effect is taken into account through proper temperature dependency of the material parameters. The evolution laws of the parameters with temperature are taken from design codes such as the Eurocode, when available, or from experimental data published in the literature.

VALIDATION OF THE MODEL

The concrete model has been validated against experimental data. The ability to capture the concrete behaviour for simple loading cases, e.g. uniaxial tension and compression, at both ambient and elevated temperature, is not demonstrated in this paper, due to the need to be concise. However experimental tests are simulated here to demonstrate the ability of the new concrete model to capture the main phenomena observed in concrete material and the ability to be used for the simulation of structural members in fire. The numerical simulations have been conducted with the software SAFIR[16].

At Ambient Temperature

A test of uniaxial tension followed by uniaxial compression on a concrete sample has been simulated using the new concrete model and the results are compared against experimental data[17], see Figure 1. The numerical results obtained with an elastoplastic concrete model are also plotted on Figure 1. The new concrete model succeeds in capturing the development of permanent strains, the degradation of the elastic properties and the stiffness recovery due to crack closure (unilateral effect), whereas elastoplastic models can only capture the development of permanent strains.

Figure 1. Numerical simulation of a uniaxial tension-compression test.

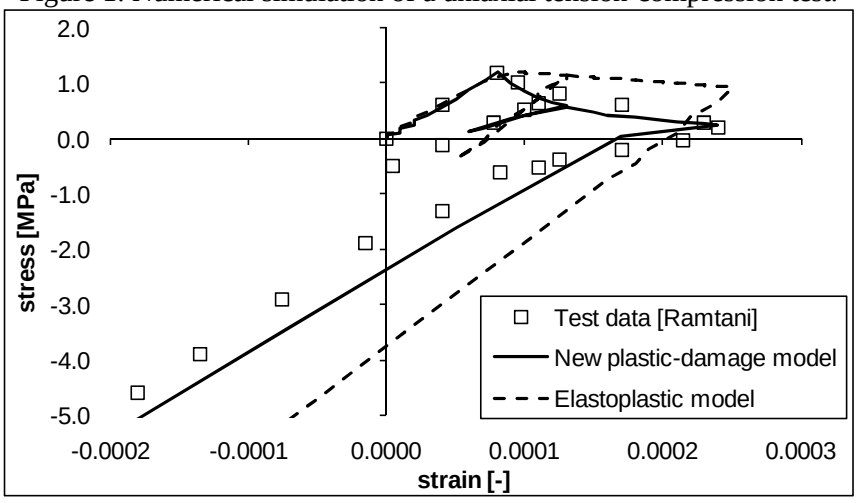

Then, the concrete model has been used in the numerical simulation of the double-edge notched (DEN) specimen experimentally studied by Nooru-Mohamed[18]. The specimen of plain concrete, which is a square plate of 200 mm long and 50 mm thick with two symmetrical notches of 25 mm by 5 mm size, is subjected to a loading path combining shear and tension at ambient temperature. The left part in Figure 2 shows the geometry of the specimen and the experimental crack pattern at the end of the test, as reported by Nooru-Mohamed. The dimensions indicated in this figure are in mm.

The loading path consists in the application of a shear force followed by tension under deformation control. A shear force P_s of 5 kN is first applied through the frame along the left-hand side of the specimen above the notch. Then, a tension loading is applied by imposing a vertical displacement d_n at the top of the specimen, while the shear force P_s remains constant equal to 5 kN. The evolution of the tensile force with the vertical displacement is recorded and the test is continued until failure of the specimen.

Due to the small thickness of the specimen, the analysis is performed in plane stress condition; therefore, shell finite elements are used in SAFIR. The mesh elements size has been taken as 5.0 mm x 5.0 mm. The specimen is made of normal weight concrete with measured compressive and tensile splitting strengths of respectively 38.4 N/mm² and 3.0 N/mm². For the used quadratic elements, the evaluation of the characteristic length l_c using the simple formula proposed by Rots[19] leads to: $l_c = A_e^{1/2} = 5$ mm. Considering a typical value of 75 N.m/m² for the crack energy in tension $\bar{G}_t$, this leads to a value of 15000 N/m² for the tensile crack energy density $g_t = \bar{G}_t / l_c$. The values of the other material parameters used in the analysis have been obtained by calibration on sample tests[11].

The values of the tensile damage parameter at the end of the simulation are plotted in the right part of Figure 2; this yields the computed crack pattern. It can be seen that the numerical simulation qualitatively captures the development of cracking in the sample.

Figure 2. Left – Geometry of the specimen and experimental crack pattern.
Right – Distribution of tensile damage at the end of the numerical simulation.

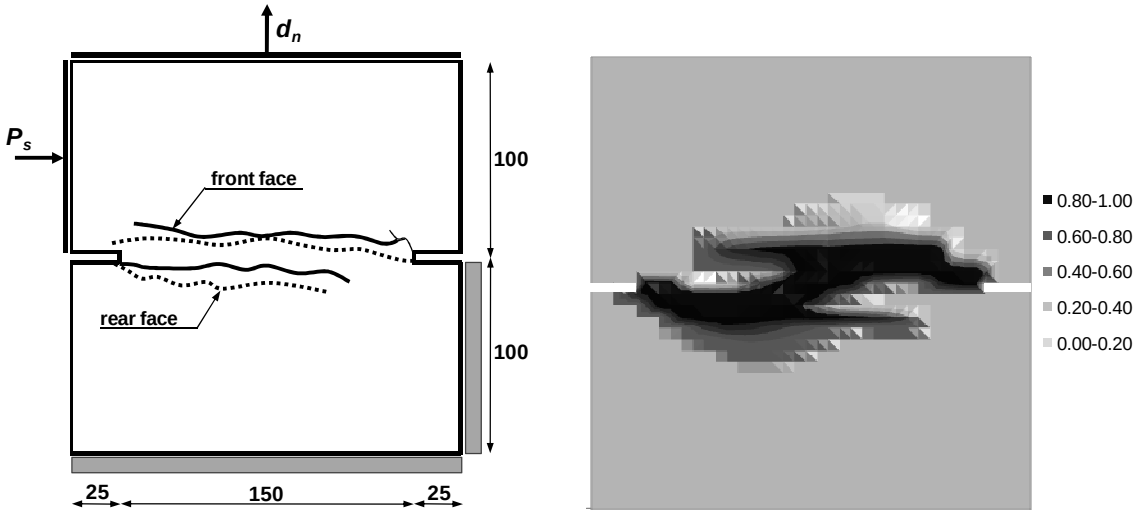

Figure 3. Measured and computed results for the mixed-mode fracture test on plain concrete

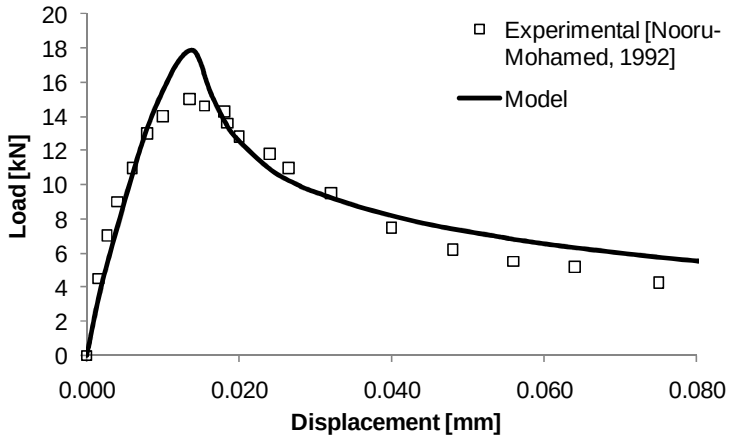

The relationship between the tensile load and the average normal displacement in the vertical direction is plotted in Figure 3. The computed results are compared with the experimental results. The computed initial stiffness fits almost perfectly the test results but the computed peak load is slightly overestimated. After the peak load, the specimen exhibits a softening response. The softening regime is well reproduced, which tends to validate the value used for the crack energy in tension. As a result, the simulation succeeds in capturing the experimental behaviour of the concrete sample subjected to shear and tension.

At High Temperature

The concrete model is validated at the structural level against experimental results on a reinforced concrete flat slab in fire. The experimental test has been carried out at BRANZ and is described in a paper by Lim et al.[20]. The tested slab is 3.30 m wide by 4.30 m long with a clear span between the supports in the long and the short directions of 4.15 m and 3.15 m, respectively. The slab is simply supported at all four edges with the edges horizontally unrestrained. The flat slab is 100 mm thickness and is reinforced by 200 mm²/m steel reinforcement in each direction. The yield strength of the steel used in the slab is 565 MPa whereas the concrete compressive strength on cylinder is 37 MPa. The concrete cover is 25 mm. The slab was subjected to ISO fire exposure for 3 hours while carrying a constant uniformly distributed live load equal to 3.0 kPa. The slab, which deformed into double curvature, survived the 3 h ISO fire exposure without collapse.

Numerical simulation of this experiment has been performed with the software SAFIR. First, the thermal analysis is conducted to determine the temperature distribution in the concrete slab during fire. The thermal properties for concrete are taken from Eurocode 1992-1-2[21]. Siliceous concrete was chosen, with a density of 2400 kg/m³ and a water content of 72 kg/m³. The emissivity was taken as 0.7 and the coefficient of convection was 25 W/m²K. Temperatures in the slab were recorded during the test at the heated surface, at the unheated surface and at 55 mm depth within the slab. Figure 4 gives the comparison between the temperatures predicted by SAFIR and the measured temperatures at these locations; predicted and measured temperatures agree well.

Figure 4. Computed and measured temperatures in the concrete slab.

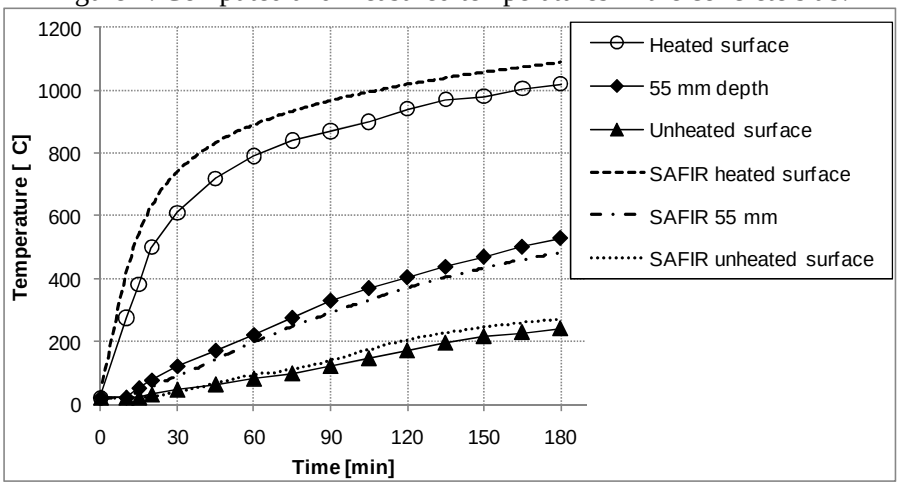

Then, the structural analysis is carried out to determine the structural behaviour of the reinforced concrete slab in fire. Shell finite elements are used for modelling the slab. Only a quarter of the full slab was modelled to take advantage of the symmetrical load and support conditions. The slab is subjected to a uniformly distributed load of 5.4 kPa which represents the sum of the self-weight, 2.4 kPa, and the live load, 3.0 kPa. This applied load of 5.4 kPa corresponds to a load ratio of approximately 0.40 for this slab. The temperature evolution in the slab is given by the SAFIR thermal analysis. The concrete model presented in this paper is used for the thermo-mechanical behaviour of concrete whereas the material model for the steel reinforcement is taken from Eurocode 1992-1-2. The concrete compressive and tensile

strength are 37.0 MPa and 1.0 MPa. The other material parameters of the concrete model are calibrated on elementary tests and no additional calibration is required on the concrete slab.

The predicted and measured vertical deflection at mid-span of the slab in fire is shown in Figure 5. Three phases can be distinguished in the evolution of the deflection: 1) a high deflection rate at the beginning of the fire due to significant thermal bowing, 2) a rather constant deflection rate during almost 120 min, and 3) a high deflection rate again in the final 30 min due to the heating of the steel rebars and the subsequent decrease in stiffness of these rebars. The simulation accurately captures the slab behaviour during the 3 hours of the fire, including the three distinct phases discussed above. The present example illustrates the ability of the new concrete model to be used in numerical simulations of structural elements in fire situation.

Figure 5. Computed (SAFIR) and measured values of the mid-span vertical deflection.

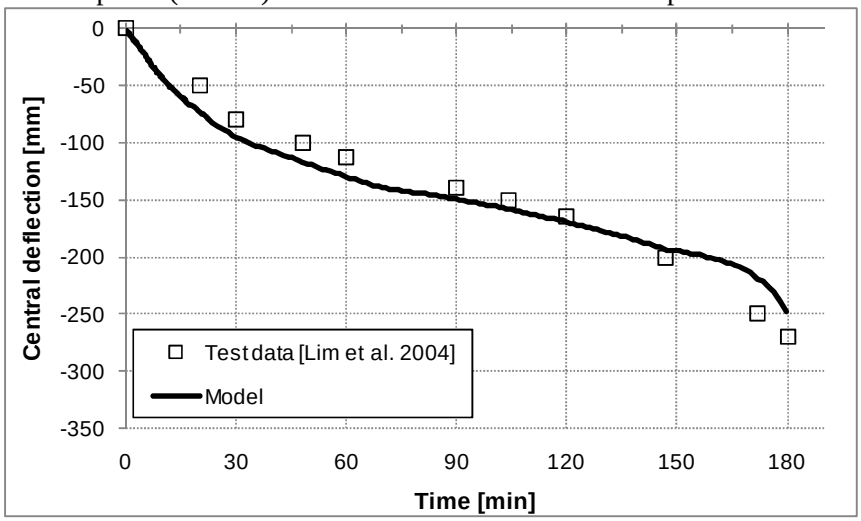

Fire Analysis – Ulster Large-Scale Fire Test

A full-scale fire test was conducted in 2010 on a steel-concrete composite floor in the framework of a project funded by the Research Fund for Coal and Steel in which six partners were involved, among which the University of Liege[22]. The objective of the test was to investigate the development of tensile membrane action in a large composite structure in which the unprotected steel beams in the central part of the floor are made of cellular beams.

The full-scale composite floor was made of cellular steel beams connected to composite slabs, see Figure 6. The compartment covers an area of 15 m by 9 m with a floor to soffit distance of 3 m. The surrounding walls of the compartment were made of normal weight concrete block works with three 3 x 1.5 m openings in the front wall. All the columns and solid beams on the opening side were protected for a standard fire of two hours using 20 mm thick fibre boards. The surrounding cellular beams were also protected using ceramic fibres, but the two central secondary beams were left unprotected. The slab was made of 51 mm deep profile of the Kingspan Multideck 50 type with a concrete cover of 69 mm on the profile, which makes a total depth of 120 mm. A steel mesh of 10 mm with a spacing of 200 mm in each direction made of S500 steel was used as reinforcement. It was located at a vertical distance of 40 mm above the steel sheets. The slab was fixed on all steel beams by means of steel studs welded on the upper flanges (full connexion).

The structure was tested under natural fire, see Figure 7. The fire load of 700 MJ/m² was achieved using 45 standard (1m x 1m x 0.5m high) wood cribs, comprising 50 mm x 50 mm x 1000 mm wooden battens, positioned evenly around the compartment, yielding a fire load of 40 kg of wood per square metre of ground area. During the fire, the floor was carrying an applied mechanical load of 3.25 kN/m^2.

Figure 6. Inside view of the compartment before the test.

Figure 7. Fire test (left) and structural elements after the fire (right).

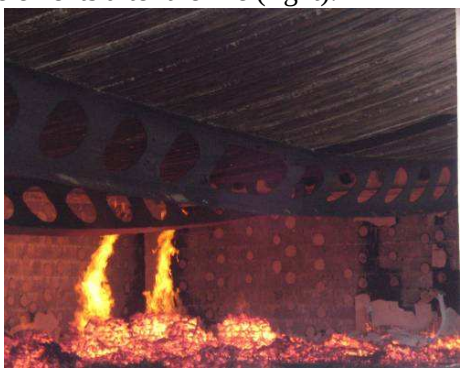

For the numerical simulation of the test, a blind approach[23] has been adopted in order to evaluate the ability of the concrete model to be used for predictive calculations. According to this approach, the temperature evolution in the compartment has been assessed by numerical simulation and the computed temperatures have then been used as input data for the SAFIR thermal analysis. The computation of the temperature evolution in the compartment is done using the software Ozone[24,25]. This software calculates the evolution of the gas temperature in a compartment under fire. Comparison between computed and measured temperatures in the compartment showed rather good agreement.

Then, the temperature evolutions in the beams and in the slab sections have been determined by 2D non linear transient thermal analyses. For the steel beams, the material properties are taken from Eurocode 1993-1-2[26] considering a convection coefficient on hot surfaces of 35.0 W/m²K, as recommended for natural fire situation[27]. The concrete slab is modelled in the thermal analysis of the steel profiles in order to take into account its capacity of absorbing heat. Siliceous concrete following the material law of Eurocode 1992-1-2[21] has been adopted with a moisture content of 72 kg/m³ and a convection coefficient on hot surfaces of 35 W/m²K. For the protected sections, the insulation material is also taken into account in the thermal analysis.

The finite element model built in SAFIR for the analysis of the mechanical behaviour of the structure uses beam elements for the steel profiles and shell elements for the composite slab, assuming full connection between the slab and the beams. The edge beams are simply supported at the location of the columns and the slab and beams are axially unrestrained. The steel profiles are made of 355 N/mm² yield strength steel, whereas the siliceous concrete used for the slab has a compressive strength of 45 N/mm². The new concrete model is used for the reinforced concrete shells using the parameters of Table 2. It was chosen to neglect the tensile strength of the concrete because, on the one hand, the structure is assumed to be cracked before the fire starts and, on the other hand, this allows to avoid defining the value of the tensile crack energy parameter, which is not easy to define at high temperature.

Table 2. Parameters of the concrete model used for the simulation.

Parameters	f_c [MPa]	f_t [MPa]	f_{c0}/f_c [-]	f_b/f_c [-]	ε_{c1} [%]	$\tilde{d}_c$ [-]	x_c [-]	υ [-]	α_g [-]
	45.0	0.0	0.30	1.16	0.25	0.30	0.19	0.20	0.25

Figure 8. Evolution of the vertical deflection of the central beam.

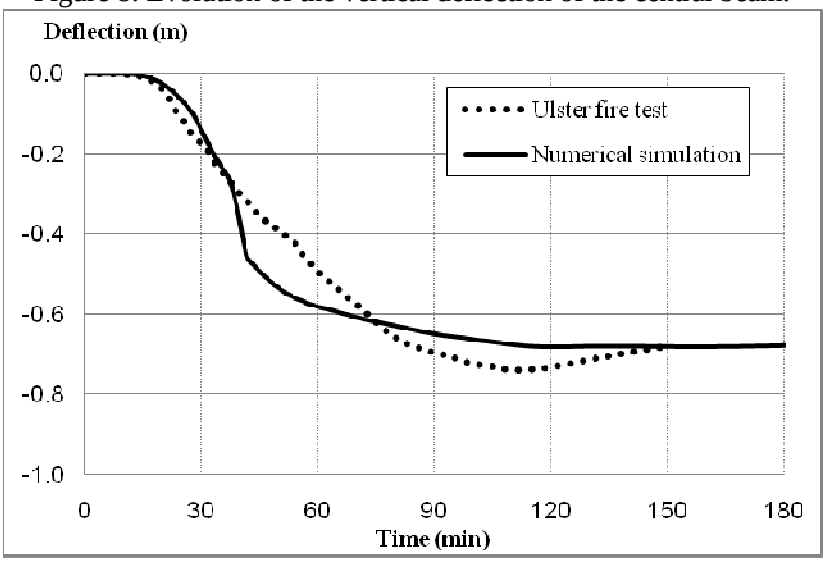

The computed results of the vertical deflection in the central steel beam are compared with the measured results in Figure 8. A good correlation is obtained between the FEM model and the real behaviour of the test; the numerical simulation qualitatively captures the evolution of the vertical deflection of the structure during the different phases of the natural fire.

Figure 9 shows the deformed shape and the distribution of membrane forces within the slab at ambient temperature and after 60 min fire exposure; in these figures, a different amplification factor has been used for plotting the deformed shape at ambient temperature (x20) and at high temperature (x2). It can be seen that the mechanism in the composite slab changes from flexural mode to tensile membrane action. After 60 min fire exposure, the unprotected steel beams have experienced web post buckling instabilities; as a result they have lost their stiffness and cannot provide support to the slab. As a consequence, the span of the slab has changed from 3.0 m to 9.0 m and membrane behaviour develops within the slab. In the central part of the slab, the steel mesh is in tension and the concrete is cracked, whereas a compressive ring develops within the concrete around the perimeter of the slab. The development of tensile membrane action in the slab is confirmed experimentally by observation of the deformed shape of the structure, see Figure 7.

The blind numerical simulation was thus able to qualitatively capture the experimental behaviour of the structure subjected to natural fire. It is noted that a better correspondence between the measured and computed results of the vertical deflection in Figure 8 could probably be obtained by adapting the parameters of the finite element model to fit with the measured values. For instance, the real temperatures measured in the sections could be used instead of the temperatures computed by a SAFIR thermal analysis. However, it was deliberately decided to fulfil the blind comparison conditions in order to get closer to the real conditions met by structural engineers who have to perform predictive calculations. Hence the obtained results give some confidence that this quite simplified model is capable of predicting the fire behaviour of a large structure in fire with a satisfying level of accuracy in the conditions of a blind comparison.

Figure 9. Deformed shape and membrane forces at ambient (left) and at high temperature (right)

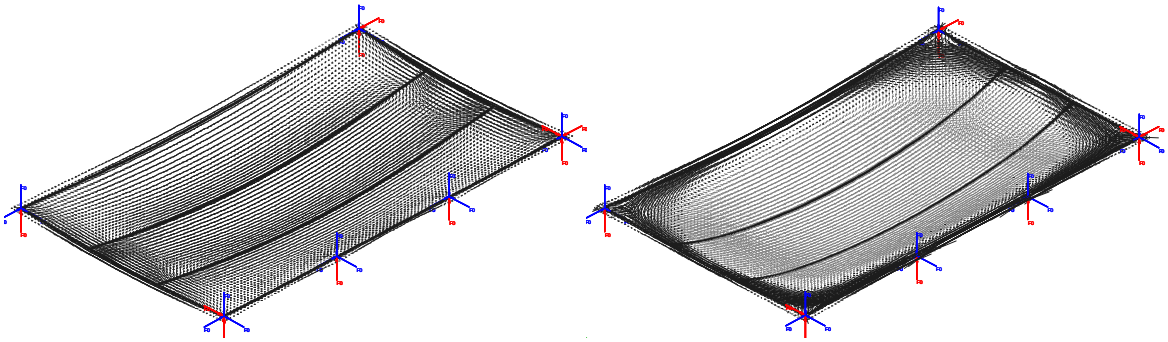

CONCLUSION

A plastic-damage concrete model has been developed and implemented in the software SAFIR for the analysis of structures in fire. The model is able to capture the phenomenological behaviour of concrete at ambient and elevated temperature and is sufficiently robust to be used in large-scale fire analysis. The model parameters can be identified by three elementary tests at ambient temperature: uniaxial compression, uniaxial tension and biaxial compression. Transient creep strain is explicitly computed and takes into account the stress-temperature history in the material.

Validation of the new model has been performed against experimental data given in the literature at ambient and elevated temperature. It has been shown that the plastic-damage model accurately captures the unilateral effect due to the closing of the tensile cracks during unloading from tension to compression, whereas elastoplastic models are unable to capture this effect. At the structural level, the model has been validated by comparison against a test carried out at BRANZ on a reinforced concrete flat slab, 3.30 m wide by 4.30 m long, subjected to ISO fire exposure during 3 hours. Finally, the ability of the model to be used in large-scale structural simulations has been illustrated by presenting the analysis of a full scale test on a composite steel-concrete slab subjected to natural fire.

REFERENCES

[1.] Lee, J. and Fenves, G., 1998. Plastic-damage model for cyclic loading of concrete structures. *J. Eng. Mech. ASCE*, pp. 892-900.

[2.] Grassl, P. and Jirasek, M., 2006. Damage-plastic model for concrete failure. *Int. J. Solids Struct.*, 43 (22-23), pp. 7166-7196.

[3.] Krätzig, W. and Polling, R., 2004. An elasto-plastic damage model for reinforced concrete with minimum number of material parameters. *Computers and Structures*, 82, pp. 1201–1215.

[4.] Carol, I., Rizzi, E. and Willam, K.J., 2001. On the formulation of anisotropic elastics degradation. II. Generalized pseudo-Rankine model for tensile damage. *Int. J. Solids Struct.* 38, pp. 519–546.

[5.] Wu, J.Y., Li, J. and Faria, R., 2006. An energy release rate-based plastic-damage model for concrete. *Int. J. Solids Struct.*, 43 (3-4), pp. 583-612.

[6.] Ju, J., 1990. Isotropic and anisotropic damage variables in continuum damage mechanics. *J. Eng. Mech. ASCE*, 116 (12), pp. 2764–2770.

[7.] Lubliner, J., Oliver, J., Oller, S. and Onate, E., 1989. A plastic-damage model for concrete. *Int. J. Solids Struct.*, 25 (3), pp. 299-326.

[8.] Ju, J., 1989. On energy-based coupled elasto-plastic damage theories: constitutive modeling and computational aspects. *Int. J. Solids Struct.*, 25, pp. 803-833.

[9.] Anderberg, Y. and Thelandersson, S., 1976. *Stress and deformation characteristics of concrete at high temperatures: 2 experimental investigation and material behavior model*, Bulletin 54, Lund Institute of Technology, Sweden.

[10.] Nechnech, W., Meftah, F. and Reynouard, J.M., 2002. An elasto-plastic damage model for plain concrete subjected to high temperatures. *Engineering structures*, 24 (5), pp. 597-611.

[11.] Gernay, T., 2012. A multiaxial constitutive model for concrete in the fire situation including transient creep and cooling down phases. Ph. D. thesis, University of Liege.

[12.] Gernay, T. and Franssen, J.-M., 2010. Consideration of transient creep in the Eurocode constitutive model for concrete in the fire situation. *Structures in Fire – Proceedings of the Sixth International Conference*, V. Kodur, J.-M. Franssen (eds.), DEStech Publications, Lancaster, pp. 784-791.

[13.] Gernay, T., 2012. Effect of transient creep strain model on the behaviour of concrete columns subjected to heating and cooling. *Fire Technology*, 48 (2), pp. 313-329.

[14.] de Borst, R. and Peeters, P., 1989. Analysis of concrete structures under thermal loading. *Computer methods in applied mechanics and engineering*, 77, pp. 293-310.

[15.] Thelandersson, S., 1987. Modelling of combined thermal and mechanical action in concrete. *ASCE J. Engrg. Mech.*, 113, pp. 893-906.

[16.] Franssen, J.-M., 2005. SAFIR, A thermal/Structural Program for Modeling Structures under Fire. *Eng J A.I.S.C.*, 42, pp. 143-158.

[17.] Ramtani, S., 1990. Contribution à la modélisation du comportement multiaxial du béton endommagé avec description du caractère unilateral. Ph. D. thesis, Univ. Paris VI E.N.S. Cachan, Paris.

[18.] Nooru-Mohamed, M.B., 1992. Mixed-mode fracture of concrete: an experimental approach. Ph. D. thesis, Delft University of Technology.

[19.] Rots, J.G., 1988. Computational modelling of concrete fracture. Ph. D. thesis, Delft University of Technology.

[20.] Lim, L., Buchanan, A., Moss, P. and Franssen, J.-M., 2004. Numerical modelling of two-way reinforced concrete slabs in fire. *Engineering Structures*, 26, pp. 1081-1091.

[21.] European Committee for Standardization, 2004. *CEN Eurocode 2 - Design of concrete structures - Part 1-2: General rules – Structural fire design.* Brussels.

[22.] Vassart, O., Bailey, C.G., Hawes, M., Nadjai, A., Simms, W.I., Zhao, B., Gernay, T. and Franssen, J.M., 2012. Large-Scale Fire Test of Unprotected Cellular Beam Acting in Membrane Action. *Proceedings of the Institution of Civil Engineers, Structures and Buildings*, 165(7), pp. 327-334.

[23.] Beard, A.N., 2000. On a priori, blind and open comparisons between theory and experiment. *Fire Safety J.*, 35(1), pp. 63-66.

[24.] Cadorin, J.F. and Franssen, J.M., 2003. A tool to design steel elements submitted to compartment fires – OZone V2. Part 1: pre- and post-flashover compartment fire model. *Fire Safety J*, 38, pp. 395-427.

[25.] Cadorin, J.F., Pintea, D., Dotreppe, J.C. and Franssen, J.M., 2003. A tool to design steel elements submitted to compartment fires – OZone V2. Part 2: Methodology and application. *Fire Safety J.*, 38, pp. 429-451.

[26.] European Committee for Standardization, 2005. *CEN Eurocode 3 - Design of steel structures - Part 1-2: General rules – Structural fire design.* Brussels.

[27.] European Committee for Standardization, 2002. *CEN Eurocode 1 – Actions on structures - Part 1-2: General actions – Actions on structures exposed to fire.* Brussels.